Figure 4.1 Summary of passive membrane properties of neurones recorded in fed, fasted and fed control group for fasted rats

A: Bar-chart showing the average membrane potential of neurones recorded from rats fed *ad libitum* (n = 47, black), rats fed *ad libitum* and housed as fasted rats (n = 50, blue) and 24-hour fasted rats (n = 52, grey).

B: Bar-chart showing the average input resistances of neurones recorded from rats fed *ad libitum* (n = 47, black), rats fed *ad libitum* and housed as fasted rats (n = 50, blue) and 24-hour fasted rats (n = 52, grey).

C: Bar-chart showing the average firing frequencies of neurones recorded from rats fed *ad libitum* (n = 47, black), rats fed *ad libitum* and housed as fasted rats (n = 50, blue) and 24-hour fasted rats (n = 52, grey).

Figure 4.2 Frequency histograms comparing passive membrane properties of neurones recorded in fed, fasted and fed control group for fasted rats

A: Frequency histograms showing the resting membrane potentials of neurones recorded from rats fed *ad libitum* (n = 47, black), rats fed *ad libitum* and housed as fasted rats (n = 50, blue) and 24-hour fasted rats (n = 52, grey). The numbers of neurones in each 5.0 mV bin size were plotted as a percentage of the population.

B: Frequency histograms comparing the range of input resistances of neurones recorded from rats fed *ad libitum* (n = 47, black), rats fed *ad libitum* and housed as fasted rats (n = 50, blue) and 24-hour fasted rats (n = 52, grey). The numbers of neurones in each 500 MΩ bin size were plotted as a percentage of the population.

C: Frequency histograms comparing the range of firing frequencies of neurones recorded from rats fed *ad libitum* (n = 47, black), rats fed *ad libitum* and housed as fasted rats (n = 50, blue) and 24-hour fasted rats (n = 52, grey). The numbers of neurones in each 0.5 Hz bin size were plotted as a percentage of the population.

Figure 4.3 **Levels of spontaneous activity and level of inactivity varied in neurones recorded in fed, fasted and fed control group for fasted rats**

Bar-chart comparing the proportion (%) of active (green) and silent (grey) neurones recorded from rats fed *ad libitum*, rats fed *ad libitum* and housed as fasted rats and 24-hour fasted rats. Note the increase in proportion of spontaneously active neurones in the control group for fasted rats (fed *ad libitum* but housed on a metal grid as fasted rats) compared to fed rats housed in standard cages.

Figure 4.4 **Comparison of membrane time-constants of neurones recorded in fed, fasted and a fed control group for fasted rats**

A: Bar-chart comparing the average membrane time-constants of neurones recorded from rats fed *ad libitum* (n = 47, black), rats fed *ad libitum* and housed as fasted rats (n = 50, blue) and 24-hour fasted rats (n = 52, grey).

B: Frequency histograms comparing the distribution of membrane time-constants of neurones recorded rats fed *ad libitum* (n = 47, black), rats fed *ad libitum* and housed as fasted rats (n = 50, blue) and 24-hour fasted rats (n = 52, grey). The numbers of neurones in each 20 ms bin size were plotted as a percentage of the population.

Figure 4.5 Characteristics and analysis of electrical properties of ARC neurones

A: Example of an action potential of ARC neurone. The amplitude of the action potential was calculated as the difference between the membrane potential measured at the threshold and the peak of the action potential (spike firing). The duration of the action potential was measured as the time difference between the rising and falling phase of the action potential at the point of threshold.

Bi: Activation of the anomalous inward rectifier (I_{an}) gave rise to a decrease in input resistance at more negative membrane potentials. The downward arrow indicated the decreased membrane response at more hyperpolarised membrane potentials relative to membrane potential response close to rest (upward arrow). Note the fast activation and the lack of inactivation of this conductance.

Bii: Activation of an A-like conductance (I_A) resulted in a delayed return to baseline following negative current injection. The duration of I_A was measured as the time between the end of current injection (marked by the first vertical dotted line) and the return of the membrane potential to the level prior to the current injection (marked by the second vertical dotted line). The amplitude of the current was measured at half the duration (line marked *).

Biii: The H-conductance (I_h) is characterized by a time- and voltage-dependent sag in the membrane response to negative current injection. The amplitude of I_h was measured by subtracting the membrane potential at the end of the negative current injection (upper dotted line) from the membrane potential following steady-state charging of the cellular membrane (lower dotted line).

Biv: The activation of the T-type calcium conductance close to the resting membrane potential resulted in a rebound depolarisation at the break of the response to negative current injection. The lower dotted line marks the resting membrane potential and the upper dotted line marks the peak of the rebound depolarisation as observed as a plateau following the action potential. To quantify the amplitude of the T-type conductance, the difference in membrane potential between resting membrane potential and the peak of the membrane depolarisation was taken.

Figure 4.6 from corel

Figure 4.7 Electrophysiological properties of clusters 1, 2 and 3

Ai: Superimposed traces from a continuous whole-cell current clamp recording of a cluster 1 neurone, showing membrane responses to a range of hyperpolarising and depolarising rectangular-wave current steps of constant increment. The arrows indicate the decreased membrane response at more hyperpolarised membrane potentials (downward arrow) relative to membrane potentials responses close to rest (upward arrow) as a result of the activation of I_{an}.

Aii: Plot of the current-voltage relationship of the neurone shown in Ai. The activation of I_{an} results in the decreased slope of the plot towards more negative membrane potentials. The arrow shows the point which the slop of the plot decreases, used as an estimation for the activation threshold for I_{an}.

Bi: Superimposed traces from a continuous whole-cell current clamp recording of a cluster 2 neurone, showing membrane responses to a range of hyperpolarising and depolarising rectangular-wave current steps of constant increment. The activation of I_{an} results in the decrease in the peak amplitude of membrane response at negative holding potentials, whereas the activation of I_A induces the delayed return to baseline following negative current injection, as indicated.

Bii: Plot of the current-voltage relationship of the neurone shown in Bi. The arrow shows the point which the slop of the plot decreases, used as an estimation for the activation threshold for I_{an}.

Ci: Superimposed traces from a continuous whole-cell current clamp recording of a cluster 3 neurone, showing membrane responses to a range of hyperpolarising and depolarising rectangular-wave current steps of constant increment. Note the lack of any distinctive subthreshold active membrane conductances.

Cii: Plot of the current-voltage relationship of the neurone shown in Ci. Note the constant slope of the plot as a result of the constant membrane resistance over the range of membrane potentials tested.

Figure 4.8 Electrophysiological properties of clusters 4, 5 and 6

Ai: Superimposed traces from a continuous whole-cell current clamp recording of a cluster 4 neurone, showing membrane responses to a range of hyperpolarising and depolarising rectangular-wave current steps of constant increment. Note the sag in the membrane response during negative current injection as a result of the activation of I_h. The amplitude of the I_h conductance was measured as the difference in membrane potential between the two dotted lines. The arrow heads shown in the I-V plot mark the decrease in activation latency (time difference between the two arrowheads) and increased amplitude of the sag at more negative membrane potentials. Closed square and open circle mark the position of the traces used to measure the instantaneous and stead-state membrane responses, respectively (see Aii).

Aii: Plot of the instantaneous (closed square) and steady-state (open circle) membrane responses of the neurone shown in Ai. The difference between the lines is indicative of the activation of I_h, which decreases the steady-state membrane response at negative holding potentials resulting in a non-linear current-voltage relationship. The arrow marks the point used to estimate the activation threshold of I_h in ARC neurones.

Bi: Superimposed traces from a continuous whole-cell current clamp recording of a cluster 5 neurone, showing membrane responses to a range of hyperpolarising and depolarising rectangular-wave current steps of constant increment. Note the sag in the membrane response during negative current injection as a result of the activation of I_h. The distance between the dotted horizontal lines indicates the amplitude of I_h. Rebound depolarisations were induced following the release of current injection contributing to the activation of a T-type calcium conductance, as indicated. Closed square and open circle mark the position of the traces used to measure the instantaneous and stead-state membrane responses, respectively (see Bii).

Bii: Plot of the instantaneous (closed square) and steady-state (open circle) membrane responses of the neurone shown in Bi. The difference between the lines is indicative of the activation of I_h, which decreases the steady-state membrane response at negative holding potentials resulting in a non-linear current-voltage relationship. The arrow marks the point used to estimate the activation threshold of I_h in ARC neurones.

Ci: Superimposed traces from a continuous whole-cell current clamp recording of a cluster 6 neurone, showing membrane responses to a range of hyperpolarising and depolarising rectangular-wave current steps of constant increment. Rebound depolarisations were induced following the release of current injection contributing to the activation of a T-type calcium conductance, as indicated. Note the absence of any other subthreshold active conductances.

Cii: Plot of the current-voltage relationship of the neurone shown in Ci. Note the linear relationship between injected current and the resulting membrane response.

Figure 4.9 Electrophysiological properties of clusters 7 and 8

Ai: Superimposed traces from a continuous whole-cell current clamp recording of a cluster 7 neurone, showing membrane responses to a range of hyperpolarising and depolarising rectangular-wave current steps of constant increment. The activation of I_{an} results in the decreased membrane response at more hyperpolarised membrane potentials (downward arrow) relative to membrane potentials responses close to rest (upward arrow). Rebound depolarisations were induced following the release of current injection contributing to the activation of a T-type calcium conductance, as indicated.

Aii: Plot of the current-voltage relationship of the neurone shown in Ai. Note the reduction in the slope of the plots towards more negative membrane potentials as a result of the activation of I_{an}, as shown with arrow.

Bi: Superimposed traces from a continuous whole-cell current clamp recording of a cluster 8 neurone, showing membrane responses to a range of hyperpolarising and depolarising rectangular-wave current steps of constant increment. The activation of I_{an} results in the decreased membrane response at more hyperpolarised membrane potentials (downward arrow) relative to membrane potentials responses close to rest (upward arrow). Rebound depolarisations were induced following the release of current injection contributing to the activation of a T-type calcium conductance, as indicated. Note the sag in the membrane response during negative current injection as a result of the activation of I_h.

Bii: Plot of the instantaneous (closed square) and steady-state (open circle) membrane responses of the neurone shown in Bi. The difference between the lines is indicative of the activation of I_h, which decreases the steady-state membrane response at negative holding potentials resulting in a non-linear current-voltage relationship. The arrow marks the point used to estimate the activation threshold of both I_h and $_{Ian}$ in ARC neurones.

Figure 4.10 Passive membrane properties and frequency histograms comparing properties of cluster 1 neurones recorded from fed, fasted and a fed control group for fasted rats

Ai: Frequency histogram plots comparing the resting membrane potentials of neurones classified as cluster 1 neurones recorded from rats fed *ad libitum* (n = 3, black), rats fed *ad libitum* and housed as fasted rats (n = 1, blue) and 24-hour fasted rats (n = 0, grey).. The numbers of neurones in each 5.0 mV bin size were plotted as a percentage of the population. Note the numbers of cluster 1 neurones recorded from all three groups of rats are low.

Aii: Bar-chart comparing the average membrane potentials of cluster 1 neurones recorded from rats fed *ad libitum* (n = 3, black), rats fed *ad libitum* and housed as fasted rats (n = 1, blue) and 24-hour fasted rats (n = 0, grey).

Bi: Frequency histogram plots comparing the input resistances of neurones recorded from rats fed *ad libitum* (n = 3, black), rats fed *ad libitum* and housed as fasted rats (n = 1, blue) and 24-hour fasted rats (n = 0, grey). The numbers of neurones in each 500 MΩ bin size were plotted as a percentage of the population.

Bii: Bar-chart comparing the average input resistances of cluster 1 neurones recorded from rats fed *ad libitum* (n = 3, black), rats fed *ad libitum* and housed as fasted rats (n=1, blue) and 24-hour fasted rats (n = 0, grey).

Ci: Frequency histogram plots comparing the firing frequencies of neurones recorded from rats fed *ad libitum* (n = 3, black), rats fed *ad libitum* and housed as fasted rats (n = 1, blue) and 24-hour fasted rats (n = 0, grey). The numbers of neurones in each 0.5 Hz bin size were plotted as percentage of population.

Cii: Bar-chart comparing the average firing frequencies of cluster 1 neurones recorded from rats fed *ad libitum* (n = 3, black), rats fed *ad libitum* and housed as fasted rats (n = 1, blue) and 24 hour fasted rats (n = 0, grey).

Figure 4.11 Passive membrane properties and frequency histograms comparing properties of cluster 2 neurones recorded from fed, fasted and a fed control group for fasted rats

Ai: Frequency histogram plots comparing the resting membrane potentials of neurones classified as cluster 2 neurones recorded from rats fed *ad libitum* (n = 2, black), rats fed *ad libitum* and housed as fasted rats (n = 1, blue) and 24-hour fasted rats (n = 2, grey). The numbers of neurones in each 5.0 mV bin size were plotted as percentage of population. Note the numbers of cluster 2 neurones recorded from all three groups are low.

Aii: Bar-chart comparing the average membrane potentials of cluster 2 neurones recorded from rats fed *ad libitum* (n = 2, black), rats fed *ad libitum* and housed as fasted rats (n = 1, blue) and 24-hour fasted rats (n = 2, grey).

Bi: Frequency histogram plots comparing the input resistances of neurones recorded from rats fed *ad libitum* (n = 2, black), rats fed *ad libitum* and housed as fasted rats (n = 1, blue) and 24-hour fasted rats (n = 2, grey) The numbers of neurones in each 500 MΩ bin size were plotted as percentage of the population.

Bii: Bar-chart comparing the average input resistances of cluster 2 neurones recorded from rats fed *ad libitum* (n = 2, black), rats fed *ad libitum* and housed as fasted rats (n = 1, blue) and 24-hour fasted rats (n = 2, grey).

Ci: Frequency histogram plots comparing the firing frequencies of neurones recorded from rats fed *ad libitum* (n = 2, black), rats fed *ad libitum* and housed as fasted rats (n = 1, blue) and 24-hour fasted rats (n = 2, grey). The numbers of neurones in each 0.5 Hz bin size were plotted as percentage of above population.

Cii: Bar-chart comparing the average firing frequencies of cluster 2 neurones recorded from rats fed *ad libitum* (n = 2, black), rats fed *ad libitum* and housed as fasted rats (n = 1, blue) and 24-hour fasted rats (n = 2, grey).

Figure 4.12 Passive membrane properties and frequency histograms comparing properties of cluster 3 neurones recorded from fed, fasted and a fed control group for fasted rats

Ai: Frequency histogram plots comparing the resting membrane potentials of neurones classified as cluster 3 neurones recorded from rats fed *ad libitum* (n = 0, black), rats fed *ad libitum* and housed as fasted rats (n = 1, blue) and 24-hour fasted rats (n = 0, grey). The numbers of neurones in each 5.0 mV bin size were plotted as percentage of the total ARC population. Note the numbers of cluster 3 neurones recorded from all three groups of rats are extremely low, further recordings are needed.

Aii: Bar-chart comparing the average membrane potentials of cluster 3 neurones recorded from rats fed *ad libitum* (n = 0, black), rats fed *ad libitum* and housed as fasted rats (n = 1, blue) and 24-hour fasted rats (n = 0, grey).

Bi: Frequency histogram plots comparing the input resistances of neurones recorded from rats fed *ad libitum* (n = 0, black), rats fed *ad libitum* and housed as fasted rats (n = 1, blue) and 24-hour fasted rats (n = 0, grey). The numbers of neurones in each 500 MΩ bin size were plotted as percentage of the total population.

Bii: Bar-chart comparing the average input resistances of cluster 3 neurones recorded from rats fed *ad libitum* (n = 0, black), rats fed *ad libitum* and housed as fasted rats (n = 1, blue) and 24-hour fasted rats (n = 0, grey).

Ci: Frequency histogram plots comparing the firing frequencies of neurones recorded from rats fed *ad libitum* (n = 0, black), rats fed *ad libitum* and housed as fasted rats (n = 1, blue) and 24-hour fasted rats (n = 0, grey). The numbers of neurones in each 0.5 Hz bin size were plotted as percentage of the total population.

Cii: Bar-chart comparing the average firing frequencies of cluster 3 neurones recorded from rats fed *ad libitum* (n = 0, black), rats fed *ad libitum* and housed as fasted rats (n = 1, blue) and 24-hour fasted rats (n = 0, grey).

Figure 4.13 Passive membrane properties and frequency histograms comparing properties of cluster 4 neurones recorded from fed, fasted and a fed control group for fasted rats

Ai: Frequency histogram plots comparing the resting membrane potentials of neurones classified as cluster 4 neurones recorded from rats fed *ad libitum* (n = 2, black), rats fed *ad libitum* and housed as fasted rats (n = 0, blue) and 24-hour fasted rats (n = 2, grey). The numbers of neurones in each 5.0 mV bin size were plotted as percentage of the total population of ARC neurones. Note the numbers of cluster 4 neurones recorded from all three groups of rats are low, thus further recordings are required.

Aii: Bar-chart comparing the average membrane potentials of cluster 4 neurones recorded from rats fed *ad libitum* (n = 2, black), rats fed *ad libitum* and housed as fasted rats (n = 0, blue) and 24-hour fasted rats (n = 2, grey).

Bi: Frequency histogram plots comparing the input resistances of neurones recorded from rats fed *ad libitum* (n = 2, black), rats fed *ad libitum* and housed as fasted rats (n = 0, blue) and 24-hour fasted rats (n = 2, grey). The numbers of neurones in each 500 MΩ bin size were plotted as a percentage of the total population.

Bii: Bar-chart comparing the average input resistances of cluster 4 neurones recorded from rats fed *ad libitum* (n = 2, black), rats fed *ad libitum* and housed as fasted rats (n = 0, blue) and 24-hour fasted rats (n = 2, grey).

Ci: Frequency histogram plots comparing the firing frequencies of neurones recorded from rats fed *ad libitum* (n = 2, black), rats fed *ad libitum* and housed as fasted rats (n = 0, blue) and 24-hour fasted rats (n = 2, grey). The numbers of neurones in each 0.5 Hz bin size were plotted as a percentage of the total population.

Cii: Bar-chart comparing the average firing frequencies of cluster 4 neurones recorded from rats fed *ad libitum* (n = 2, black), rats fed *ad libitum* and housed as fasted rats (n = 0, blue) and 24-hour fasted rats (n = 2, grey).

Figure 4.14 Passive membrane properties and frequency histograms comparing properties of cluster 5 neurones recorded from fed, fasted and a fed control group for fasted rats

Ai: Frequency histogram plots comparing the resting membrane potentials of neurones classified as cluster 5 neurones recorded from rats fed *ad libitum* (n = 17, black), rats fed *ad libitum* and housed as fasted rats (n = 15, blue) and 24-hour fasted rats (n = 14, grey). The numbers of neurones in each 5.0 mV bin size were plotted as percentage of the total population recorded for each group.

Aii: Bar-chart comparing the resting membrane potentials of cluster 5 neurones recorded from rats fed *ad libitum* (n = 17, black), rats fed *ad libitum* and housed as fasted rats (n = 15, blue) and 24-hour fasted rats (n = 14, grey).

Bi: Frequency histogram plots comparing the input resistances of neurones recorded from rats fed *ad libitum* (n = 17, black), rats fed *ad libitum* and housed as fasted rats (n = 15, blue) and 24-hour fasted rats (n = 14, grey). The numbers of neurones in each 500 MΩ bin size were plotted as percentage of the total population recorded for each group.

Bii: Bar-chart comparing the average input resistances of cluster 5 neurones recorded from rats fed *ad libitum* (n = 17, black), rats fed *ad libitum* and housed as fasted rats (n = 15, blue) and 24-hour fasted rats (n = 14, grey).

Ci: Frequency histogram plots comparing the firing frequencies of neurones recorded from rats fed *ad libitum* (n = 17, black), rats fed *ad libitum* and housed as fasted rats (n = 15, blue) and 24-hour fasted rats (n = 14, grey). The numbers of neurones in each 0.5 Hz bin size were plotted as percentage of the total population recorded for each group.

Cii: Bar-chart comparing the average firing frequencies of cluster 5 neurones recorded from rats fed *ad libitum* (n = 17, black), rats fed *ad libitum* and housed as fasted rats (n = 15, blue) and 24-hour fasted rats (n = 14, grey).

Figure 4.15 Passive membrane properties and frequency histograms comparing properties of cluster 6 neurones recorded from fed, fasted and a fed control group for fasted rats

Ai: Frequency histogram plots comparing the membrane potentials of neurones classified as cluster 6 neurones recorded from rats fed *ad libitum* (n = 12, black), rats fed *ad libitum* and housed as fasted rats (n = 11, blue) and 24-hour fasted rats (n = 12, grey). The numbers of neurones in each 5.0 mV bin size were plotted as percentage of the total population recorded for each group.

Aii: Bar-chart comparing the average membrane potentials of cluster 6 neurones recorded from rats fed *ad libitum* (n = 12, black), rats fed *ad libitum* and housed as fasted rats (n = 11, blue) and 24-hour fasted rats (n = 12, grey).

Bi: Frequency histogram plots comparing the input resistances of neurones recorded from rats fed *ad libitum* (n = 12, black), rats fed *ad libitum* and housed as fasted rats (n = 11, blue) and 24-hour fasted rats (n = 12, grey). The numbers of neurones in each 500 MΩ bin size were plotted as percentage of the total population recorded for each group.

Bii: Bar-chart comparing the average input resistances of cluster 6 neurones recorded from rats fed *ad libitum* (n = 12, black), rats fed *ad libitum* and housed as fasted rats (n = 11, blue) and 24-hour fasted rats (n = 12, grey).

Ci: Frequency histogram plots comparing the firing frequencies of neurones recorded from rats fed *ad libitum* (n = 12, black), rats fed *ad libitum* and housed as fasted rats (n = 11, blue) and 24-hour fasted rats (n = 12, grey). The numbers of neurones in each 0.5 Hz bin size were plotted as percentage of the total population recorded for each group.

Cii: Bar-chart comparing the average firing frequencies of cluster 6 neurones recorded from rats fed *ad libitum* (n = 12, black), rats fed *ad libitum* and housed as fasted rats (n = 11, blue) and 24-hour fasted rats (n = 12, grey).

Figure 4.16 Passive membrane properties and frequency histograms comparing properties of cluster 7 neurones recorded from fed, fasted and a fed control group for fasted rats

Ai: Frequency histogram plots comparing the resting membrane potentials of neurones classified as cluster 7 neurones recorded from rats fed *ad libitum* (n = 4, black), rats fed *ad libitum* and housed as fasted rats (n = 7, blue) and 24-hour fasted rats (n = 8, grey). The numbers of neurones in each 5.0 mV bin size were plotted as percentage of the total population recorded for each group.

Aii: Bar-chart comparing the resting membrane potentials of cluster 7 neurones recorded from rats fed *ad libitum* (n = 4, black), rats fed *ad libitum* and housed as fasted rats (n = 7, blue) and 24-hour fasted rats (n = 8, grey).

Bi: Frequency histogram plots comparing the input resistances of neurones recorded from rats fed *ad libitum* (n = 4, black), rats fed *ad libitum* and housed as fasted rats (n = 7, blue) and 24-hour fasted rats (n = 8, grey). The numbers of neurones in each 500 MΩ bin size were plotted as percentage of the total population recorded for each group.

Bii: Bar-chart comparing the average input resistances of cluster 7 neurones recorded from rats fed *ad libitum* (n = 4, black), rats fed *ad libitum* and housed as fasted rats (n = 7, blue) and 24-hour fasted rats (n = 8, grey).

Ci: Frequency histogram plots comparing the firing frequencies of neurones recorded from rats fed *ad libitum* (n = 4, black), rats fed *ad libitum* and housed as fasted rats (n = 7, blue) and 24-hour fasted rats (n = 8, grey). The numbers of neurones in each 0.5 Hz bin size were plotted as percentage of the total population recorded for each group.

Cii: Bar-chart comparing the average firing frequencies of cluster 7 neurones recorded from rats fed *ad libitum* (n = 4, black), rats fed *ad libitum* and housed as fasted rats (n = 7, blue) and 24-hour fasted rats (n = 8, grey).

Figure 4.17 Passive membrane properties and frequency histograms comparing properties of cluster 8 neurones recorded from fed, fasted and a fed control group for fasted rats

Ai: Frequency histogram plots comparing the membrane potentials of neurones classified as cluster 8 neurones recorded from rats fed *ad libitum* (n = 7, black), rats fed *ad libitum* and housed as fasted rats (n = 14, blue) and 24-hour fasted rats (n = 14, grey). The numbers of neurones in each 5.0 mV bin size were plotted as percentage of the total population recorded for each group.

Aii: Bar-chart comparing the average membrane potentials of cluster 8 neurones recorded from rats fed *ad libitum* (n = 7, black), rats fed *ad libitum* and housed as fasted rats (n = 14, blue) and 24-hour fasted rats (n = 14, grey).

Bi: Frequency histogram plots comparing the input resistances of neurones recorded from rats fed *ad libitum* (n = 7, black), rats fed *ad libitum* and housed as fasted rats (n = 14, blue) and 24-hour fasted rats (n = 14, grey). The numbers of neurones in each 500 MΩ bin size were plotted as percentage of the total population recorded for each group.

Bii: Bar-chart comparing the average input resistances of cluster 8 neurones recorded from rats fed *ad libitum* (n = 7, black), rats fed *ad libitum* and housed as fasted rats (n = 14, blue) and 24-hour fasted rats (n = 14, grey).

Ci: Frequency histogram plots comparing the firing frequencies of neurones recorded from rats fed *ad libitum* (n = 7, black), rats fed *ad libitum* and housed as fasted rats (n = 14, blue) and 24-hour fasted rats (n = 14, grey). The numbers of neurones in each 0.5 Hz bin size were plotted as percentage of the total population recorded for each group.

Cii: Bar-chart comparing the average firing frequencies of cluster 8 neurones recorded from rats fed *ad libitum* (n = 7, black), rats fed *ad libitum* and housed as fasted rats (n = 14, blue) and 24-hour fasted rats (n = 14, grey).

Figure 4.1

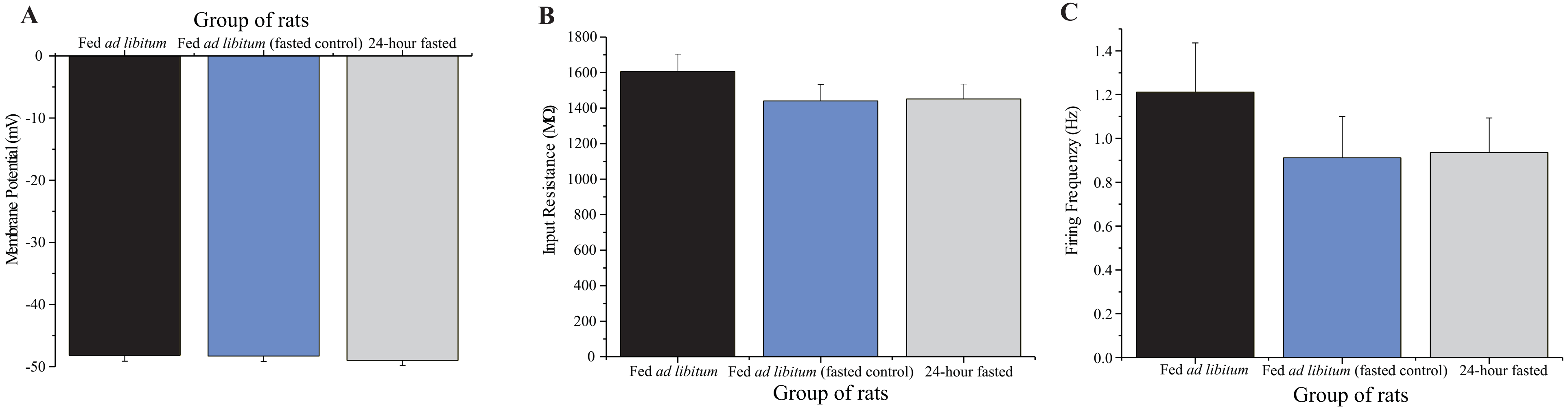

Figure 4.2

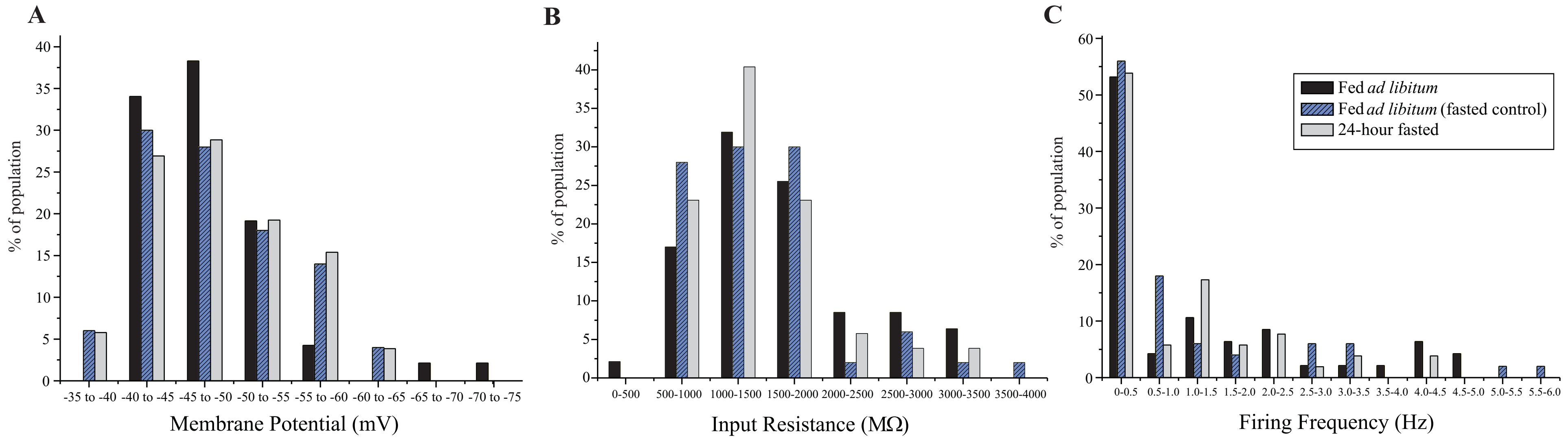

Figure 4.3

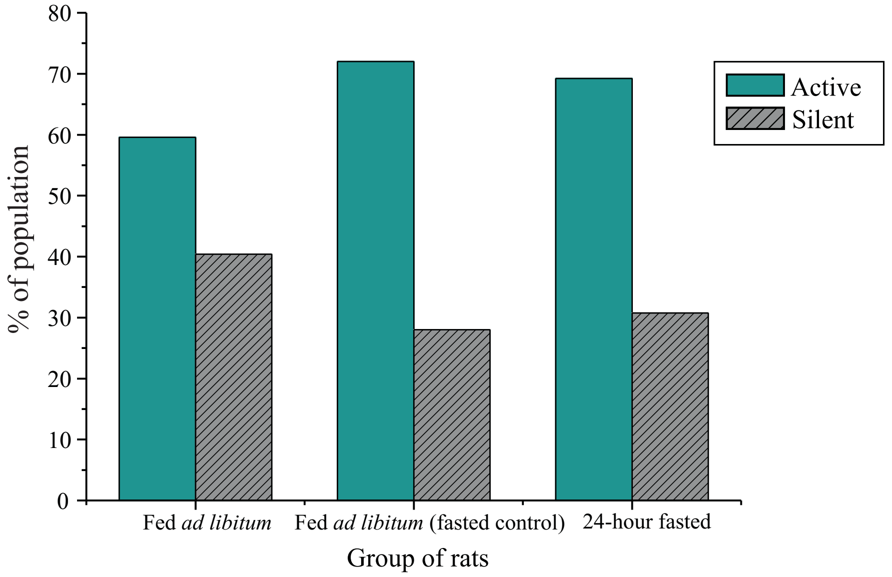

Figure 4.4

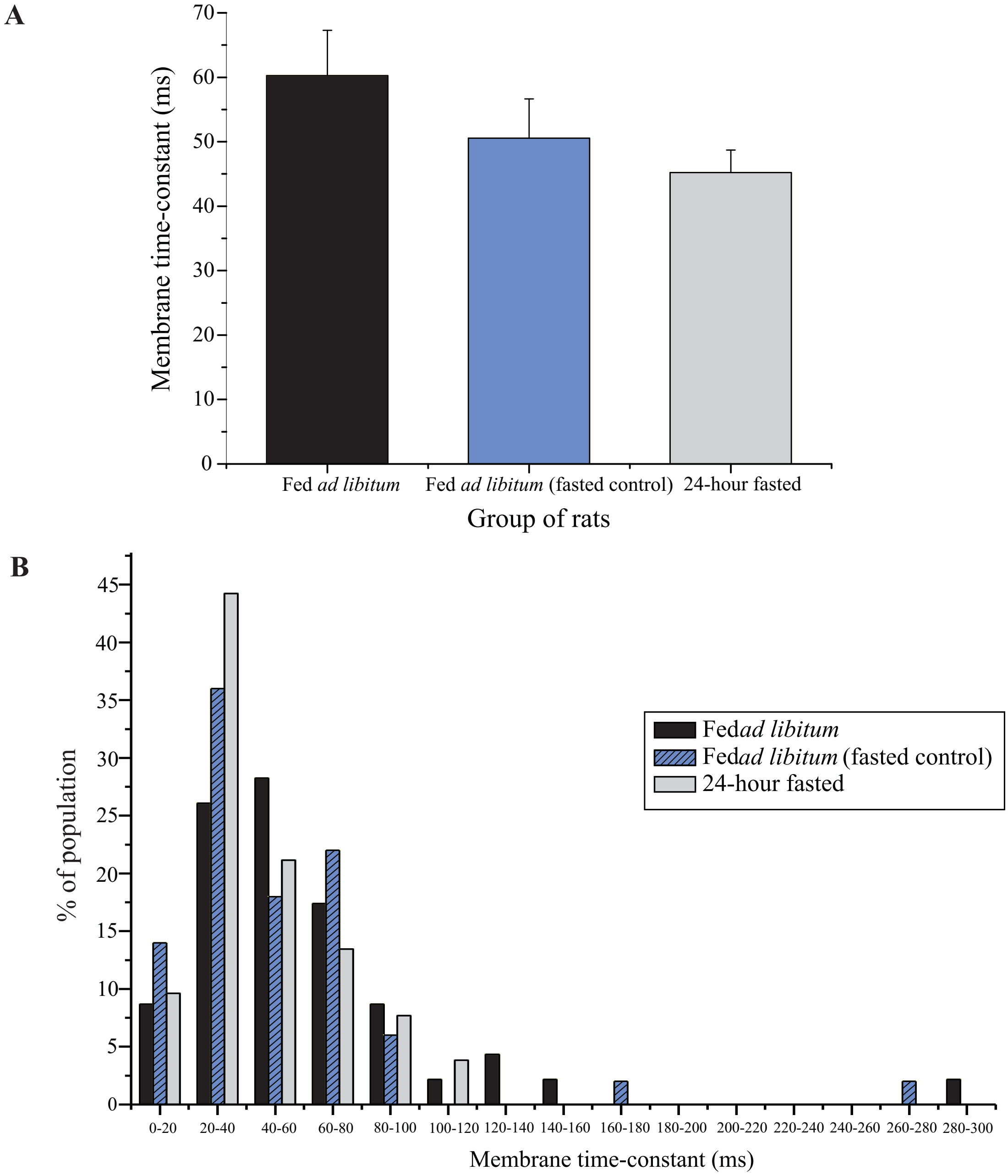

Figure 4.5

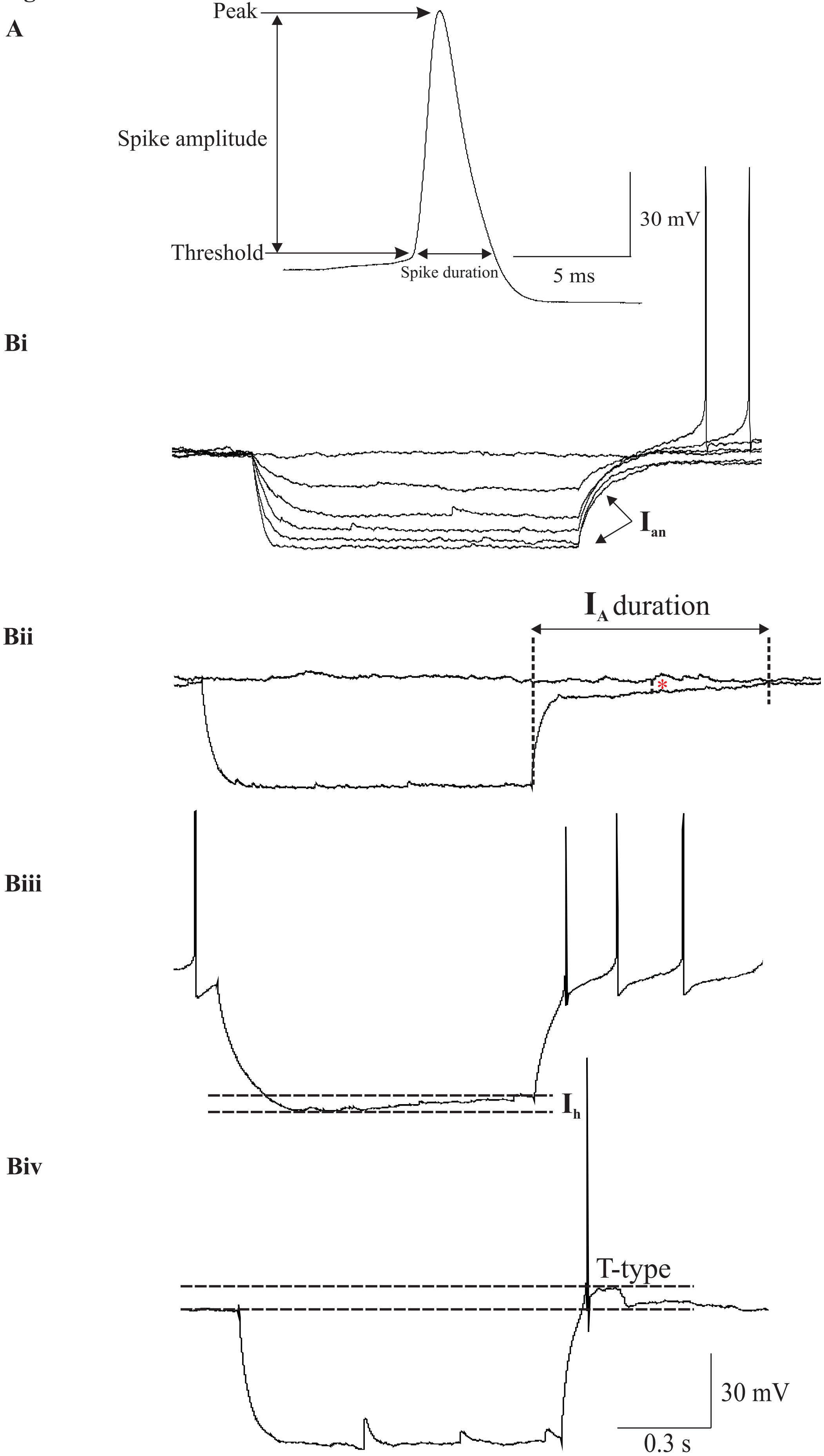
A
Peak
Spike amplitude
Threshold
Spike duration
30 mV
5 ms
Bi
I_{an}
Bii
I_A duration
*
Biii
I_h
Biv
T-type
30 mV
0.3 s

Figure 4.6

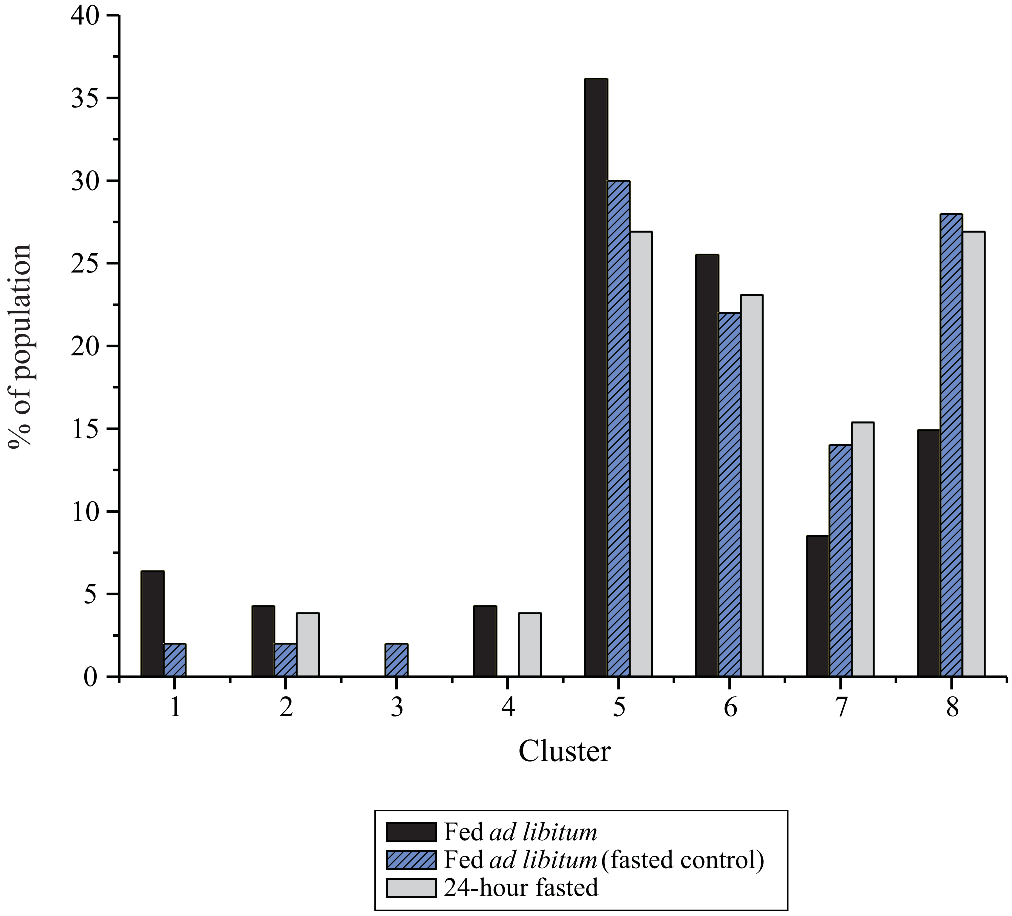

Figure 4.6 Differential distributions of ARC neurones expressing unique combinations of subthreshold active conductances (clusters) in fed, fasted and a fed control group for fasted rats

Neurones were classified into 8 electrophysiological clusters based upon their expression of unique or unique combinations of subthreshold active conductances. The bar-chart summarises the distribution of these 8 electrophysiological clusters expressed as a percentage of the population of neurones recorded from, recorded from rats fed *ad libitum* (n = 47, black), rats fed *ad libitum* and housed as fasted rats (n = 50, blue) and 24-hour fasted rats (n = 52, grey).

Figure 4.7

Ai Cluster 1

Aii

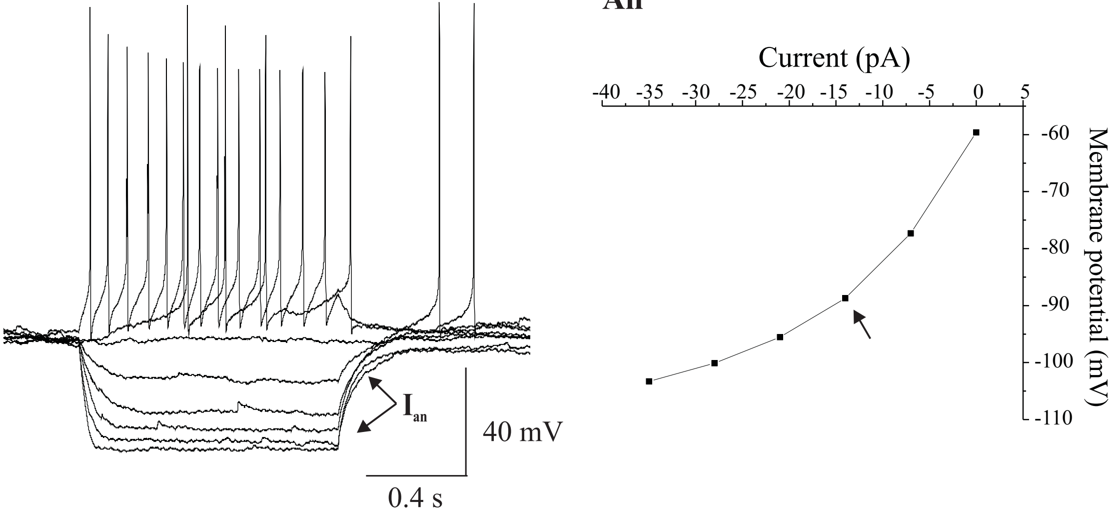

Bi Cluster 2

Bii

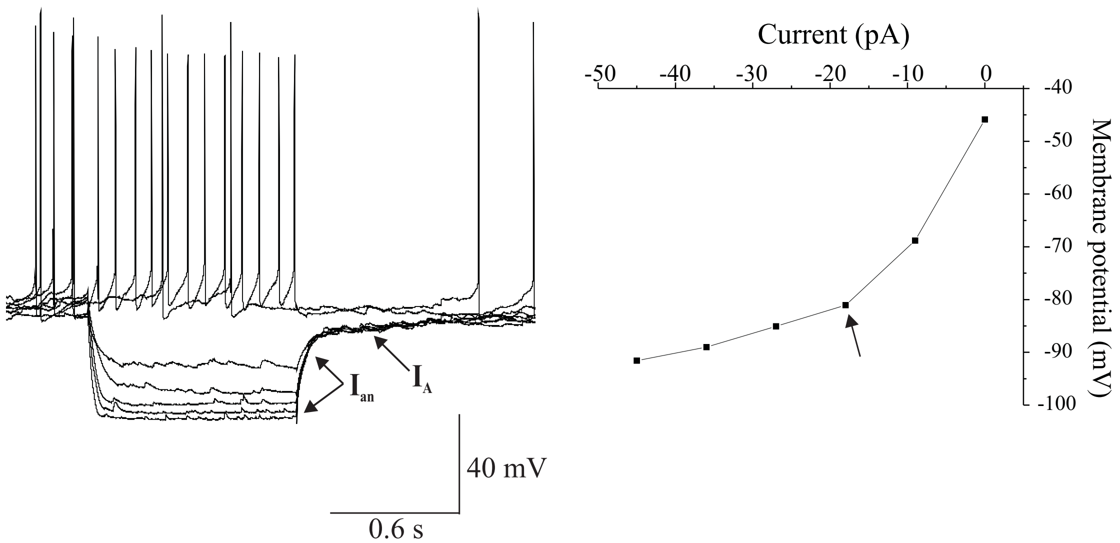

Ci Cluster 3

Cii

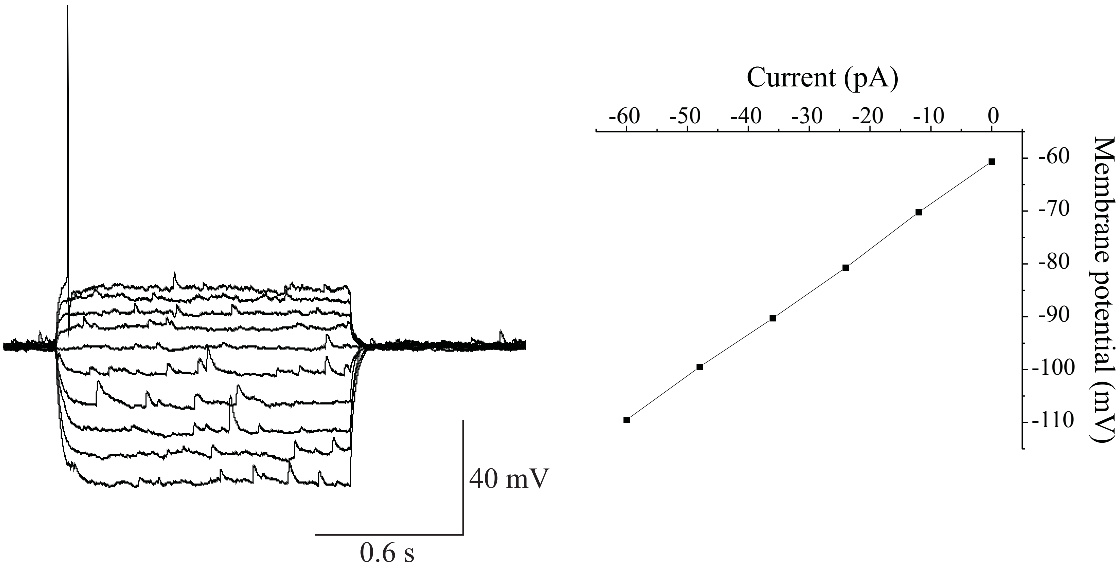

Figure 4.8

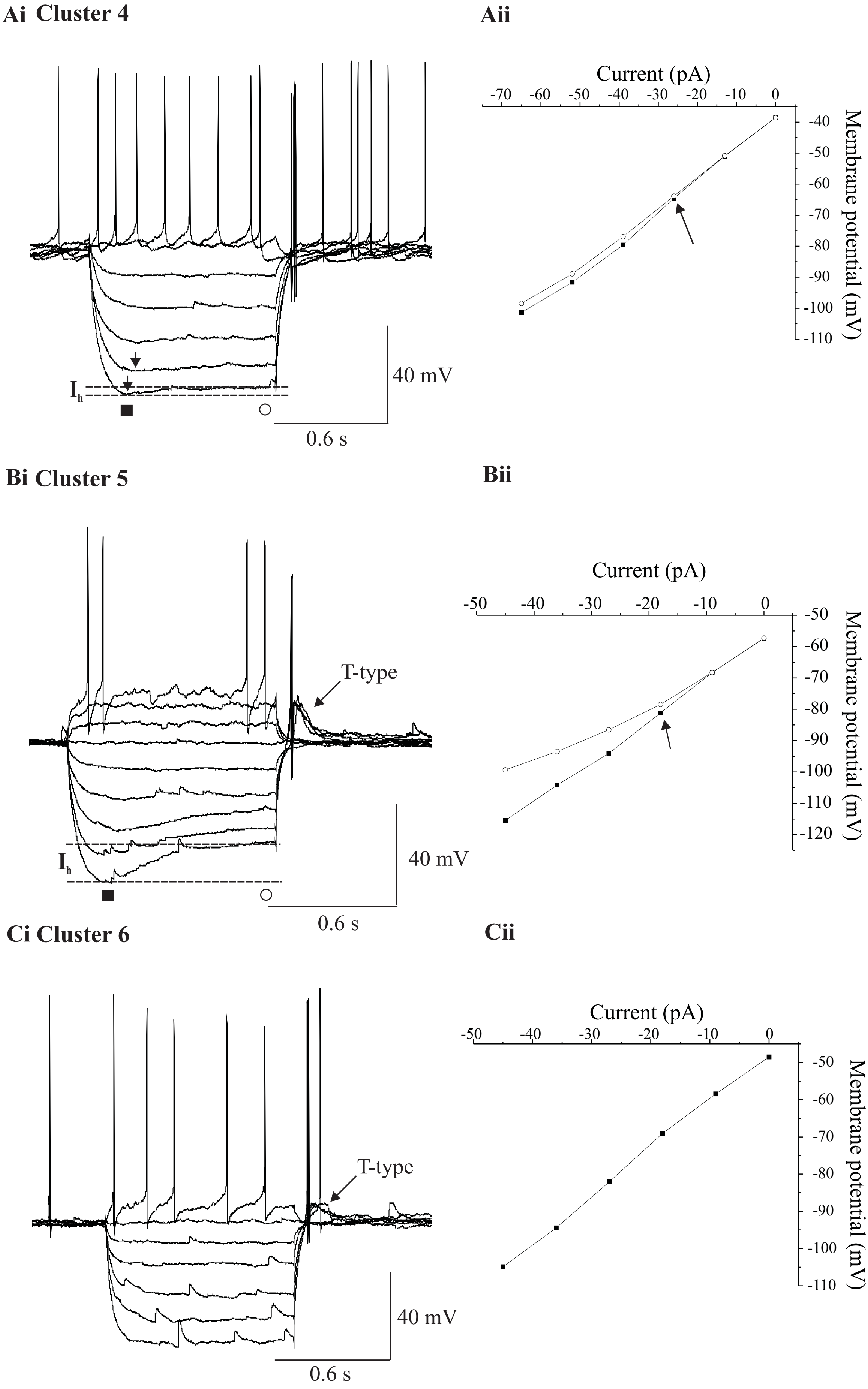
Ai Cluster 4
Aii
I_h
40 mV
0.6 s
Current (pA)
-70 -60 -50 -40 -30 -20 -10 0
Membrane potential (mV)
-40 -50 -60 -70 -80 -90 -100 -110
Bi Cluster 5
Bii
T-type
I_h
40 mV
0.6 s
Current (pA)
-50 -40 -30 -20 -10 0
Membrane potential (mV)
-50 -60 -70 -80 -90 -100 -110 -120
Ci Cluster 6
Cii
T-type
40 mV
0.6 s
Current (pA)
-50 -40 -30 -20 -10 0
Membrane potential (mV)
-50 -60 -70 -80 -90 -100 -110

Figure 4.9

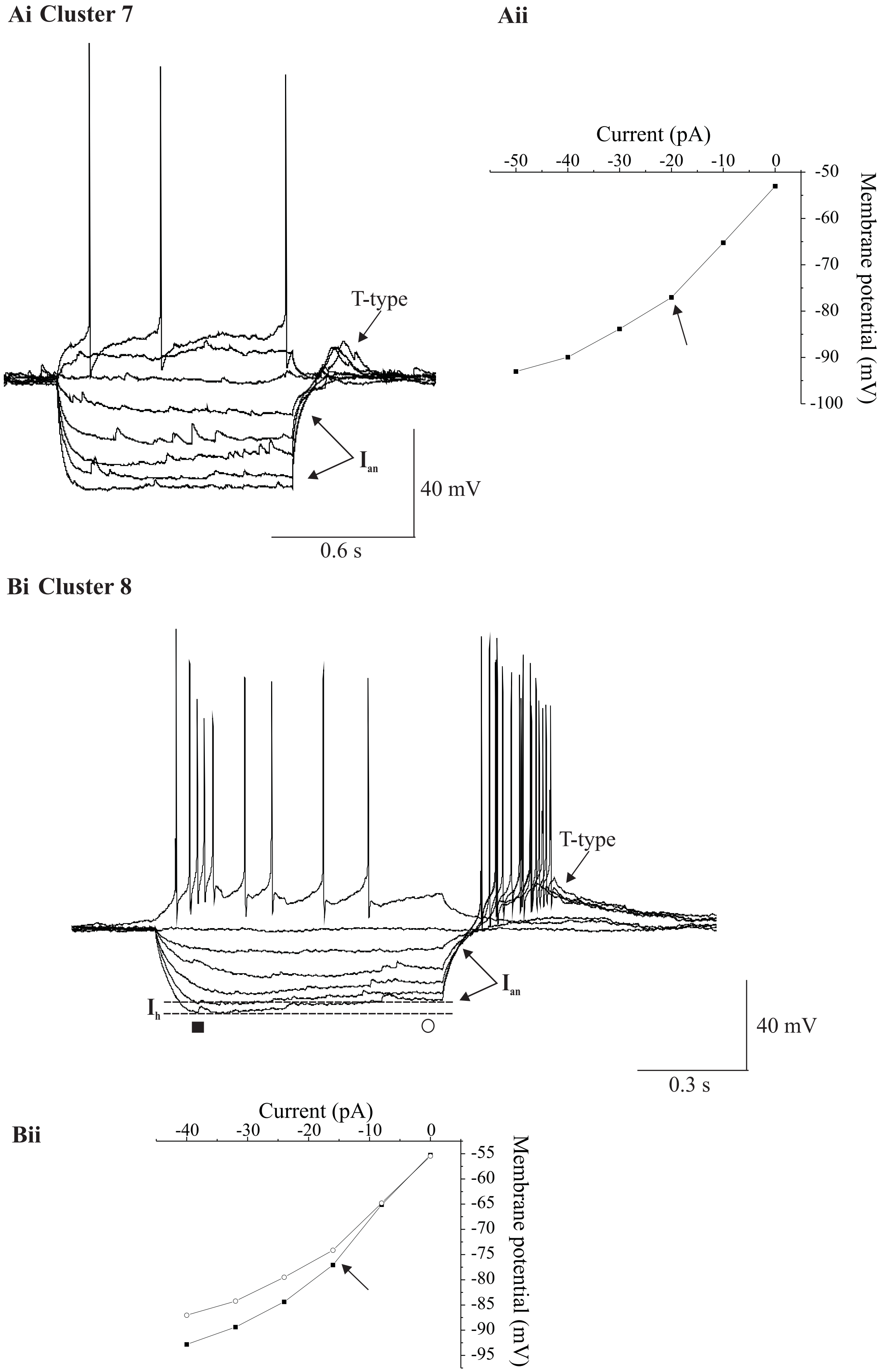
Ai Cluster 7
Aii
T-type
I_{an}
40 mV
0.6 s
Current (pA)
-50
-40
-30
-20
-10
0
-50
-60
-70
-80
-90
-100
Membrane potential (mV)
Bi Cluster 8
T-type
I_{an}
I_h
■
○
40 mV
0.3 s
Bii
Current (pA)
-40
-30
-20
-10
0
-55
-60
-65
-70
-75
-80
-85
-90
-95
Membrane potential (mV)

Figure 4.10: Cluster 1

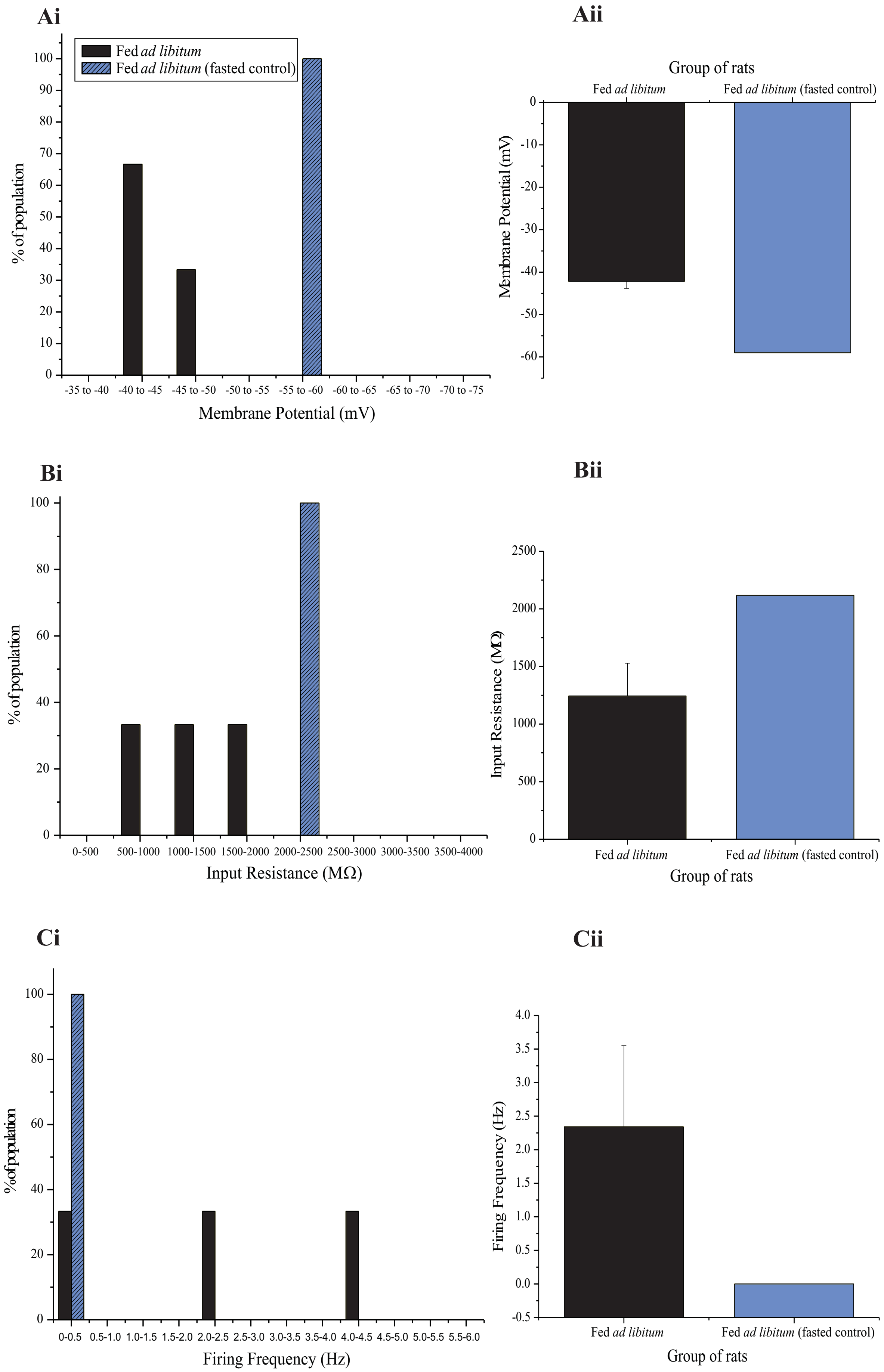

Figure 4.11: Cluster 2

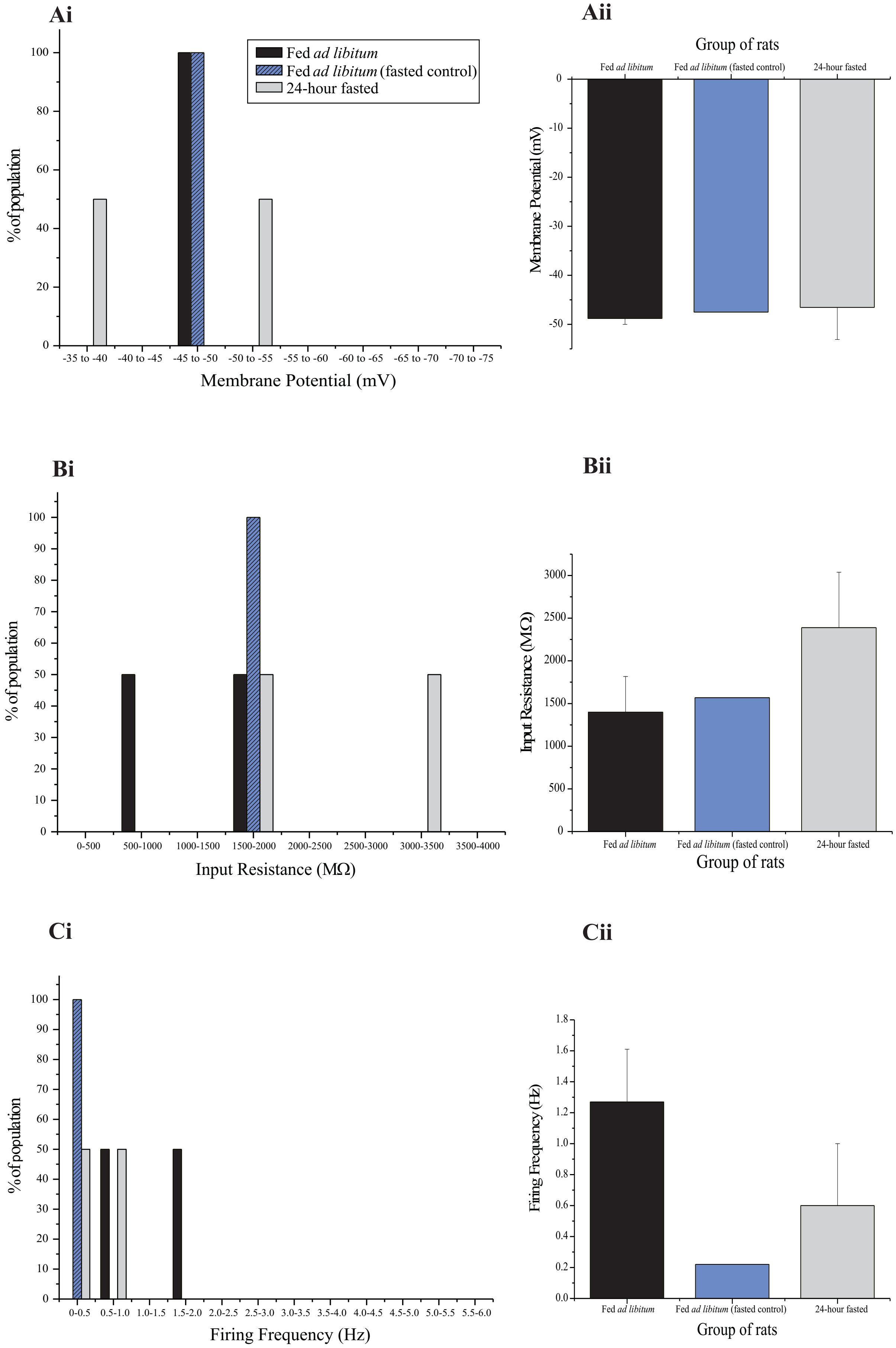

Figure 4.12: Cluster 3

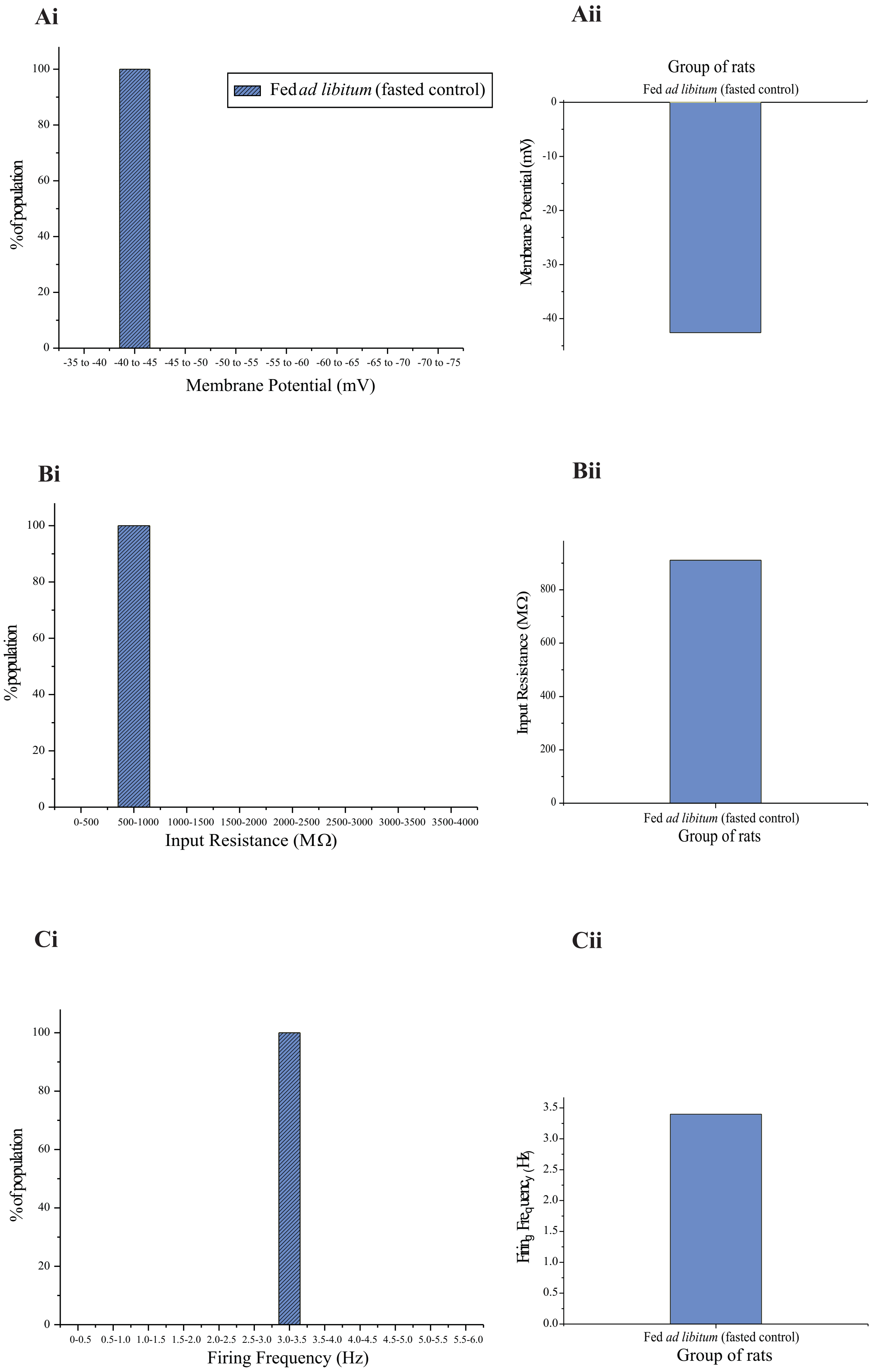

Figure 4.13: Cluster 4

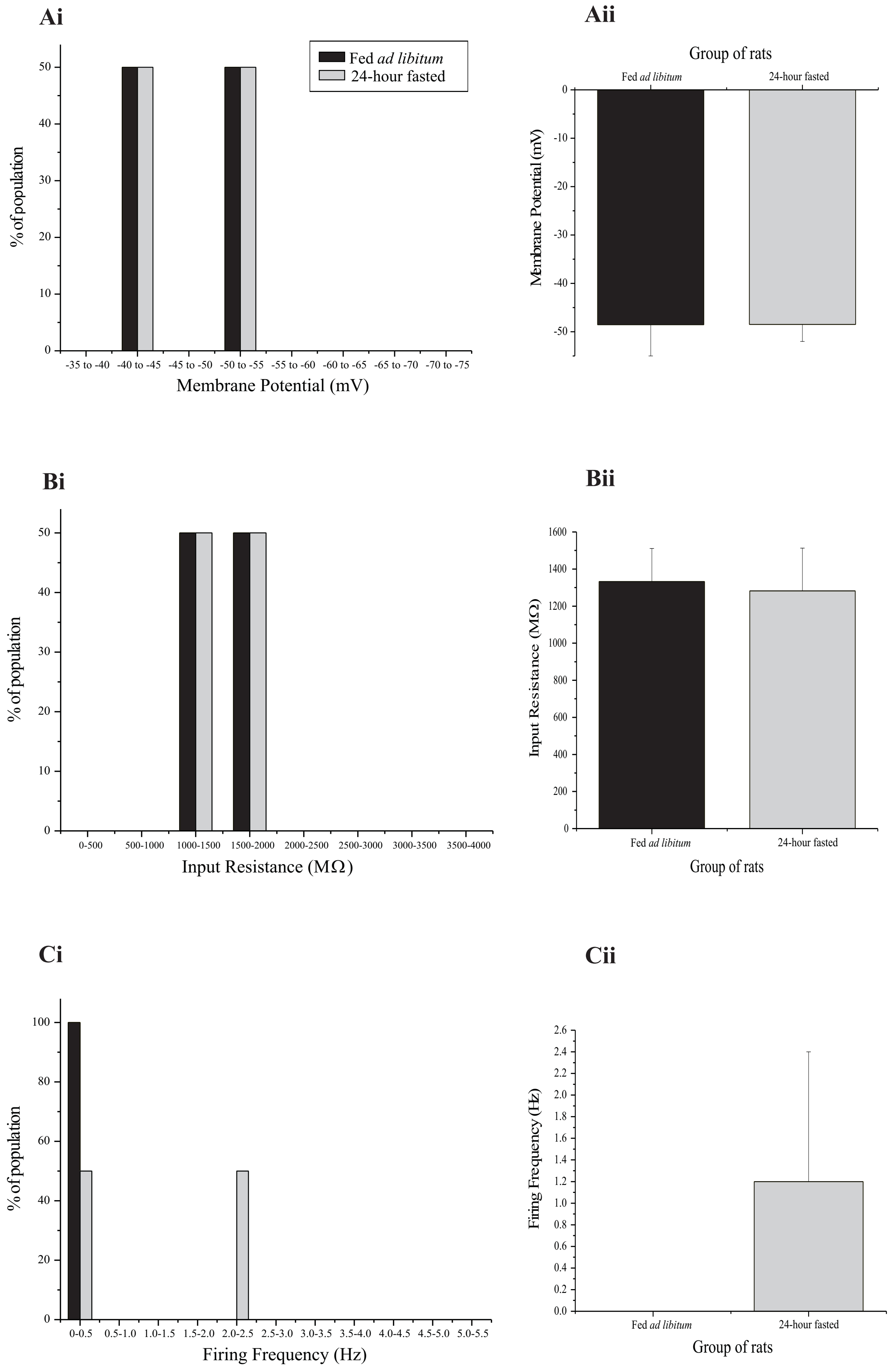

Figure 4.14: Cluster 5

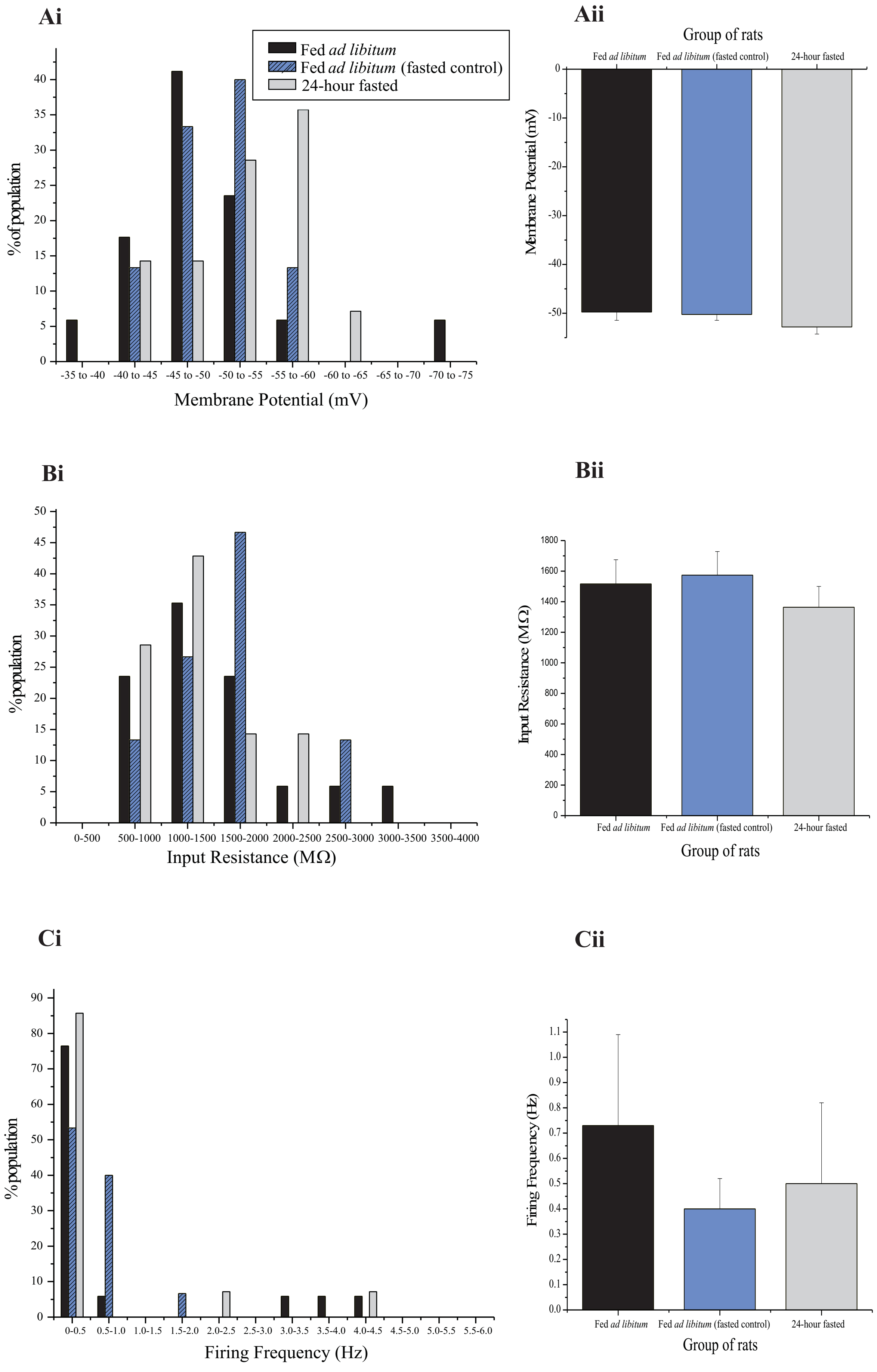

Figure 4.15: Cluster 6

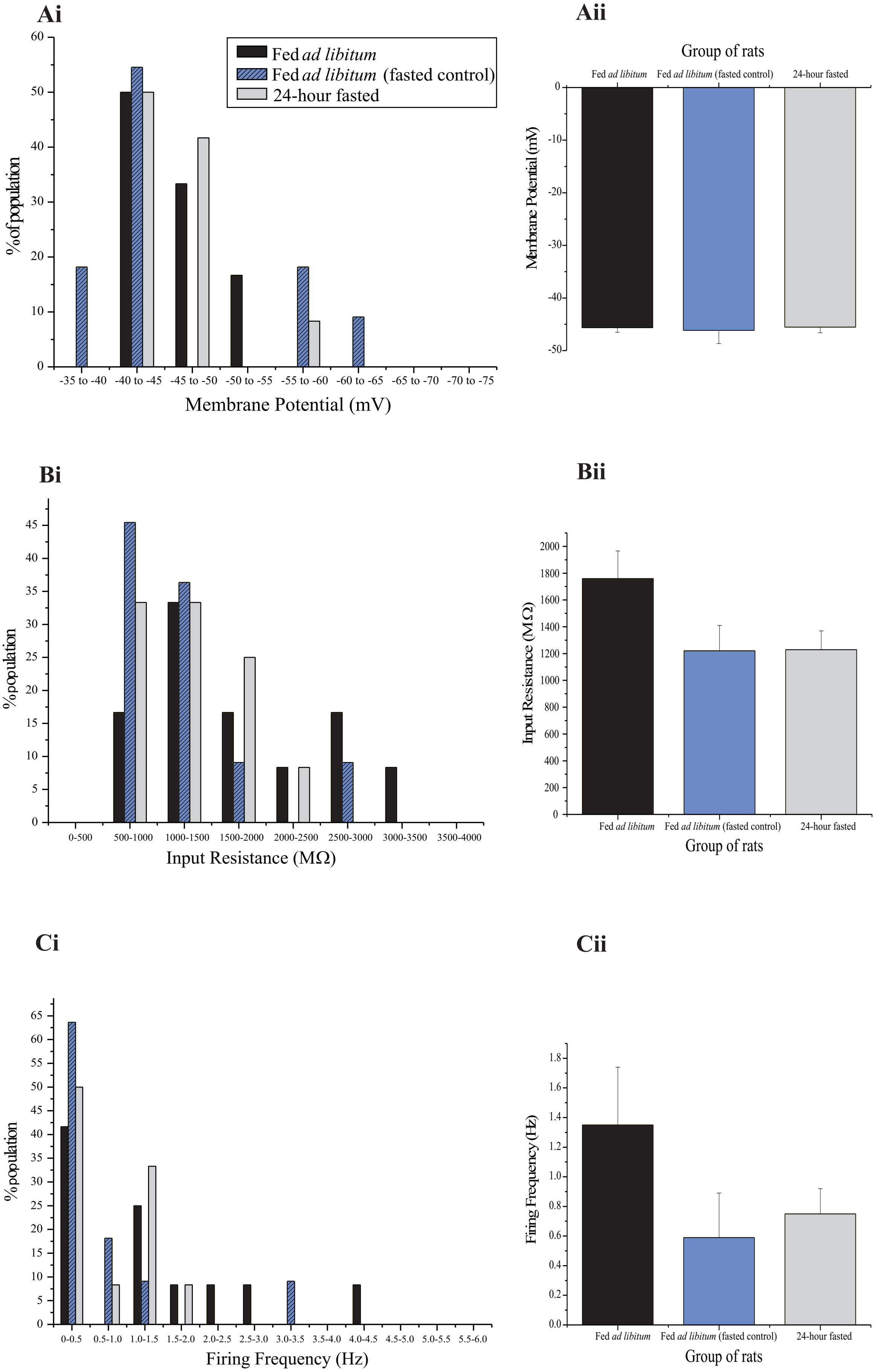

Figure 4.16: Cluster 7

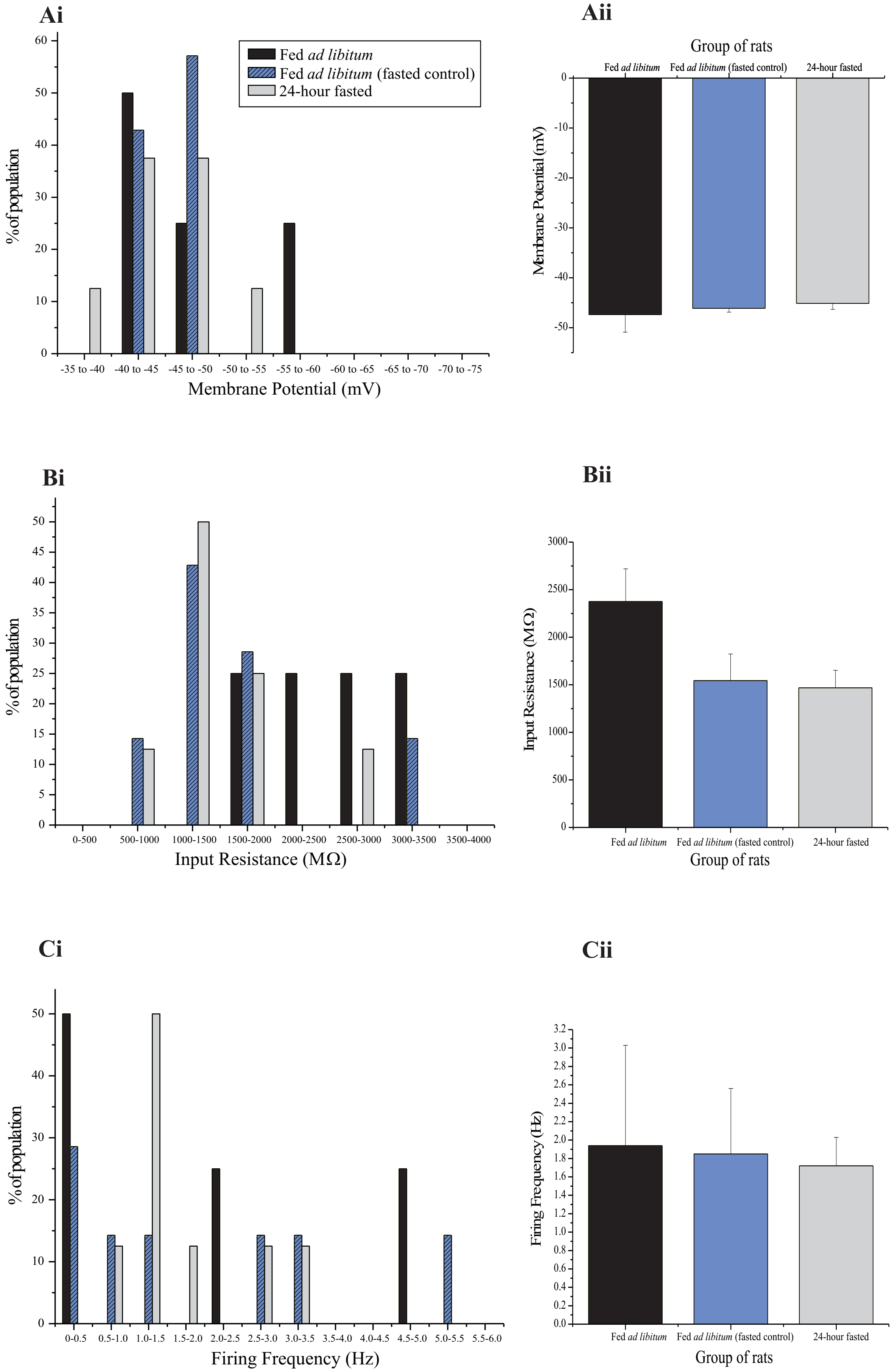

Figure 4.17: Cluster 8